GEOCHEMISTRY

Long-term rise in riverine dissolved organic carbon concentration is predicted by electrolyte solubility theory

Donald T. Monteith[1]*, Peter A. Henrys[1], Jakub Hruška[2,3], Heleen A. de Wit[4,5], Pavel Krám[2,3], Filip Moldan[6], Maximilian Posch[7], Antti Räike[8], John L. Stoddard[9], Ewan M. Shilland[10,11,12], M. Gloria Pereira[1], Chris D. Evans[13]

Copyright © 2023 The Authors, some rights reserved; exclusive licensee American Association for the Advancement of Science. No claim to original U.S. Government Works. Distributed under a Creative Commons Attribution License 4.0 (CC BY).

The riverine dissolved organic carbon (DOC) flux is of similar magnitude to the terrestrial sink for atmospheric CO_2, but the factors controlling it remain poorly determined and are largely absent from Earth system models (ESMs). Here, we show, for a range of European headwater catchments, that electrolyte solubility theory explains how declining precipitation ionic strength (IS) has increased the dissolution of thermally moderated pools of soluble soil organic matter (OM), while hydrological conditions govern the proportion of this OM entering the aquatic system. Solubility will continue to rise exponentially with declining IS until pollutant ion deposition fully flattens out under clean air policies. Future DOC export will increasingly depend on rates of warming and any directional changes to the intensity and seasonality of precipitation and marine ion deposition. Our findings provide a firm foundation for incorporating the processes dominating change in this component of the global carbon cycle in ESMs.

INTRODUCTION

The global riverine carbon (C) flux, of circa 1.7 to 2.7 Pg year^{-1} (*1*), is similar in magnitude to C uptake by both the land surface and the oceans (*2*). In regions where wetter, and/or cooler, climates have led to the development of organic-rich soils, dissolved organic carbon (DOC) is often the dominant form of the exported C that also includes particulate and inorganic forms (*3*). DOC concentrations and fluxes in waters draining these systems are highly dynamic and have increased over much of northern Europe and northeastern America over the past three to four decades (*4*–*6*). These changes are important not only for the lateral export of C to the oceans per se but also for the ecological and biogeochemical structure and functioning of aquatic ecosystems because DOC provides a substrate for heterotrophic respiration (*7*) and limits aquatic primary productivity by attenuating photosynthetically active radiation (*8*). From a societal perspective, rising DOC concentrations in upland drinking water sources are a major concern for water companies with legal requirements to maintain predisinfection DOC concentrations at low levels and are thus faced with mounting water treatment costs (*9*) and uncertainty over future treatment infrastructure needs.

A range of process-based models have been developed to evaluate drivers of DOC variation and change in temperate (*10*), boreal (*11*), and Arctic (*12*) environments. While valuable for the development of scientific understanding, most are highly parameterized, require substantial site-specific calibration, and therefore have limited potential for upscaling. Although some have attempted to capture the processes determining longer-term DOC concentration change (*13*, *14*), this has arguably been addressed more effectively by statistically based attribution, in which rates of change in DOC have been linked to surrogates of acid deposition (*4*, *6*, *15*) and hydrological metrics such as discharge (*16*). Correlative model structures, however, can be challenging to interpret mechanistically. Ultimately, the appropriate attribution of environmental controls on DOC concentration requires that all key processes influencing variation, from episodic to seasonal to interannual time scales, are realistically represented, integrated, and shown to be applicable across a range of environmental settings. A robust, holistic, parsimonious, and transferable representation of DOC dynamics has thus remained elusive but is urgently needed, not only to constrain the land surface components of Earth system models and develop clearer insights into potential climate change feedbacks (*2*) but also to improve the understanding of the impacts of environmental change on aquatic biodiversity and drinking water supply.

The organic substances contributing to DOC in surface waters have various origins and range widely in molecular size and chemical characteristics (*17*). However, the dissolved organic matter (OM) most associated with DOC increases, sometimes referred to as "humic substances," is characterized by colored, hydrophobic, high–molecular weight compounds indicative of terrestrial (i.e., allochthonous) sources. Isotopic analysis of this type of DOC normally indicates very recent provenance (terrestrial primary production) and generation (via OM decomposition) close to the soil surface,

[1]UK Centre for Ecology and Hydrology, Lancaster Environment Centre, Library Avenue, Bailrigg, Lancaster LA1 4AP, UK. [2]Czech Geological Survey, Klárov 3, 11821 Prague, Czech Republic. [3]Global Change Research Institute, Czech Academy of Sciences, Bělidla 986/4a, 603 00 Brno, Czech Republic. [4]Norwegian Institute for Water Research (NIVA), Oslo, Norway. [5]Centre for Biogeochemistry in the Anthropocene, Department of Biosciences, Section for Aquatic Biology and Toxicology, University of Oslo, Oslo, Norway. [6]IVL Swedish Environmental Research Institute, Box 530 21, 400 14 Göteborg, Sweden. [7]International Institute for Applied Systems Analysis (IIASA), A-2361 Laxenburg, Austria. [8]Finnish Environment Institute (SYKE), P.O.Box 140, FI-00790 Helsinki, Finland. [9]US EPA, Corvallis, OR 97333, USA. [10]Environmental Change Research Centre, UCL, Gower Street, London WC1E 6BT, UK. [11]Life Sciences, Natural History Museum, Cromwell Road, London, SW7 5BD, UK. [12]School of Biological and Behavioural Sciences, Queen Mary University of London, Mile End Road, London E1 4NS, UK. [13]UK Centre for Ecology and Hydrology, Environment Centre Wales, Deiniol Road, Bangor, LL57 2UW, UK.
*Corresponding author. Email: donm@ceh.ac.uk

Downloaded from https://www.science.org at University College London on January 23, 2023

even in waters draining peatlands, provided that these are relatively undisturbed (*18*, *19*). Microbial decomposition, a seasonally varying temperature-dependent process (*20*, *21*), renders OM available for leaching, while the rate of OM mobilization as DOC, as well as its export to surface waters, is influenced by the chemical characteristics of leachate, which determine OM solubility, and hydrological pathways (*22*, *23*) dependent on topographic, soil, and geological properties and both current and antecedent precipitation. In organomineral soils, a notable amount of DOC may percolate into mineral layers where it becomes subject to adsorption/desorption processes and molecular transformation (*24*, *25*).

We developed a simple mathematical simulation approach to test the extent to which it is possible to explain episodic, seasonal, and long-term variation in DOC in long-term headwater records on the basis of just three linked processes: (i) thermal control of terrestrial OM decomposition rates, (ii) the effect of atmospheric deposition on soil OM solubility, and (iii) the influence of hydrological variation on DOC transport from soils to waters. Of these processes, the mechanism(s) linking deposition to solubility have arguably remained the least resolved to date and thus provide the main focus of the current study.

Rates of change in DOC concentration in long-term hydrochemical records tend to correlate negatively with rates of change in indicators of acid deposition, e.g., sulfate and chloride concentration in surface waters (*6*) and bulk deposition (*15*), with effects most acute for waters with lower base cation concentrations (*4*). The solubility of humic substances is known to be linked to the extent of complexation with protons and metal ions (*26*, *27*), and the correlative observations therefore suggest that terrestrial OM solubility is increasing in response to either, or both, a reduction in soil acidity and/or soil water ionic strength (IS), hypotheses also supported by laboratory and plot-scale manipulation experiments on DOC concentrations in the organic horizons of a range of soils (*28*–*31*).

Nevertheless, surface waters recovering from acidification do not always show correlations between DOC and water pH. For example, substantial increases in DOC were reported in two upland streams in the Czech Republic in the absence of any clear change in streamwater pH (*32*), although the increases were strongly, and inversely, correlated with streamwater IS. Similar observations were made for a range of headwater streams in the Adirondack region of the United States (*33*). Both studies concluded that reductions in soil water IS were likely to be the dominant factor influencing the DOC increases, but many other more recently published analyses of long-term DOC trends continue to overlook IS as a primary control (*34*–*39*). Furthermore, the IS of runoff itself may be considered a flawed indicator of the effects of changes in atmospheric deposition on DOC because, in the examples above, measurements of DOC and IS made essentially on the same water samples cannot be considered independent. Streamwater IS can also be influenced by changes in the proportional contributions to runoff from relatively ion-rich groundwater. Hence, during wetter periods, for example, lower IS due to baseflow dilution may be accompanied by higher DOC concentrations resulting from a switch to shallower lateral flow paths. It is therefore difficult to fully separate cause-effect relationships between streamwater DOC concentration and IS from hydrological covariance, although the Czech study also demonstrated similar DOC-IS relationships within soil water (*32*), which would be independent of this possible flow-path effect.

Unfortunately, long-term records of soil water IS that are colocated with headwater monitoring stations are rare and tend to be too plot-specific for catchment-scale assessments. We therefore tested the IS-based hypothesis within our simulations by applying the electrical conductivity (EC) of locally monitored bulk deposition, a robust and easy-to-measure surrogate for IS, as an indirect predictor of changing soil water IS (Materials and Methods). The Debye-Hückel theory (*40*) implies that the natural logarithm of ion activity in dilute solutions is inversely proportional to the square root of IS. On this basis, we reasoned that if IS is the primary factor regulating soil OM solubility and fluctuations in the EC of water leaching the upper soil organic layer are dominated by the atmospheric input of ions, then for any site, (i) the natural logarithm of DOC concentration (*lnDOC*) will vary in inverse proportion to the square root of precipitation EC ($\sqrt{EC}$); (ii) when both precipitation EC and *lnDOC* are expressed as proportions of long-term site medians (i.e., $lnDOC_{prop}$ and EC_{prop}), then $\sqrt{EC_{prop}}$ and $lnDOC_{prop}$ should be related by a linear function with a slope of approximately −1 and an intercept of 1; and (iii) fits will be maximized when precipitation EC has first been averaged (precipitation-weighted) over a period representing the average response time of a catchment's soluble OM pool to change in deposition inputs. While proportional variation in precipitation EC will be an imperfect surrogate for proportional variation in the EC of water percolating through surficial soil organic layers, we considered it to be a valid predictor of longer-term changes in soil water IS and the most robust predictor of a solubility effect available to us.

We collated multidecadal hydrochemical records with varying degrees of acid sensitivity (as determined by base cation concentration) from eight long-established headwater monitoring stations to develop our DOC simulations and test the hypothesis that IS represents a common control on soil OM solubility. The sites were drawn from the Czech Republic, Sweden, Norway, and the United Kingdom, with a requirement that locally recorded daily discharge and precipitation EC measurements, and either locally recorded or modeled daily mean air temperature data were available (see the Supplementary Materials). Half of these sites, Lysina, Pluhuv Bor, Allt a'Mharcaidh, and the River Etherow showed negative relationships between discharge and streamwater EC, thus demonstrating the limitation of using the latter as a causal predictor of the deposition-driven solubility effect.

Site-specific models were fitted by first determining the (precipitation weighted-average) smoothing window for precipitation EC_{prop} that maximized the variance in $lnDOC_{prop}$ explained by the relationship described above (and see Methods and Materials). We then fitted an effect of antecedent air temperature, a surrogate for soil temperature, and a two-component discharge effect representing the (nonlinear) influence of discharge on the day of sampling to explain the residual variance. The antecedent period of smoothing for air temperature, the temperature coefficient, and the two discharge coefficients were then adjusted iteratively until model fits (determined by the variance explained) were maximized. However, the coefficient and intercept for the $\sqrt{EC_{prop}}$ variable were fixed at −1 and 1, respectively, for all sites. The final model structure is presented as Eq. 3 in Materials and Methods.

Downloaded from https://www.science.org at University College London on January 23, 2023

RESULTS AND DISCUSSION

Implications of model fits for catchment process understanding

The final model fits provided highly effective simulations of DOC variation over time scales ranging from intersample to seasonal and interannual (Fig. 1), while the consistency of the final selection of antecedent smoothing windows and model coefficients across stations (Table 1) emphasized the wide-scale applicability and potential transferability of the approach. Optimal antecedent smoothing windows for temperature were significantly shorter (9 to 74 days) than those for antecedent precipitation EC (110 to 600 days). Because soil temperatures are likely to lag air temperatures by a few days, the short antecedent air temperature windows indicated that the effect of soil temperature on DOC production was relatively immediate at most sites, while the longer windows for the smoothing of the deposition EC effect indicated a more temporally smoothed influence of atmospherically deposited solutes on OM solubility.

Air temperature coefficients conformed with the range of incubation temperature quotients often associated with OM decomposition (Q_{10} range = 1.3 to 2.7) (*41*, *42*) and were positively correlated with the proportion of the catchment covered by peat and peaty gley soils, i.e., the main predominantly anoxic organic soil classes (R^2 = 0.65, P = 0.01). With the exception of Storgama, all sites showed similar positive and curvilinear relationships between DOC and either discharge or the logarithm of discharge. DOC was most sensitive to changing discharge in the lower flow ranges and leveled out at higher flows. The absence of a detectable hydrological influence at Storgama is likely to reflect the catchment's thin and sparsely distributed soil cover (*43*).

The models explained between 31 and 81% (mean = 56%) of the overall variance in DOC, while the slopes of the linear temporal trends in modeled DOC ranged between 67 and 115% (mean = 97%) of those of the observed DOC. The poorest model fit was achieved for the River Etherow where, unlike the other sites, discharge data were only available for a station several kilometers downstream (see the Supplementary Materials). Most variance was explained for sites where variation in DOC was dominated by either discharge (highly episodic) or temperature (strongly seasonal), but precipitation EC was clearly most important in explaining the linear trend (Fig. 2) despite the coefficient and intercept for this variable being fixed across all sites. Precipitation EC was the only variable capable of independently explaining most of the overall modeled DOC concentration slope at any site. This therefore provides strong evidence that the electrolyte solubility effect, as described by Debye-Hückel theory, represents a fundamental and universal control on terrestrial OM dynamics.

Agreement between observed and fitted DOC trends was optimized by the inclusion of one or both of the other variables, thus demonstrating their importance as either synergistic or antagonistic factors, but in the absence of a long-term reduction in precipitation EC, neither temperature nor discharge (separately or in combination) were capable of accounting for any more than a small fraction of the observed long-term DOC increase (Fig. 2). Furthermore, the model implied that the recent decline in discharge at Lysina would have resulted in an overall reduction in DOC over the past three decades had the atmospheric ion flux not fallen considerably over the same period.

The discrete influence of the three variables on modeled DOC concentration across the full variable range for each site is provided in Fig. 3 (A to C), while the influence each variable exerted on modeled DOC concentrations over the monitoring period is shown in Fig. 3 (D to F). The effect of precipitation EC on overall variance in DOC concentration is of similar magnitude to the

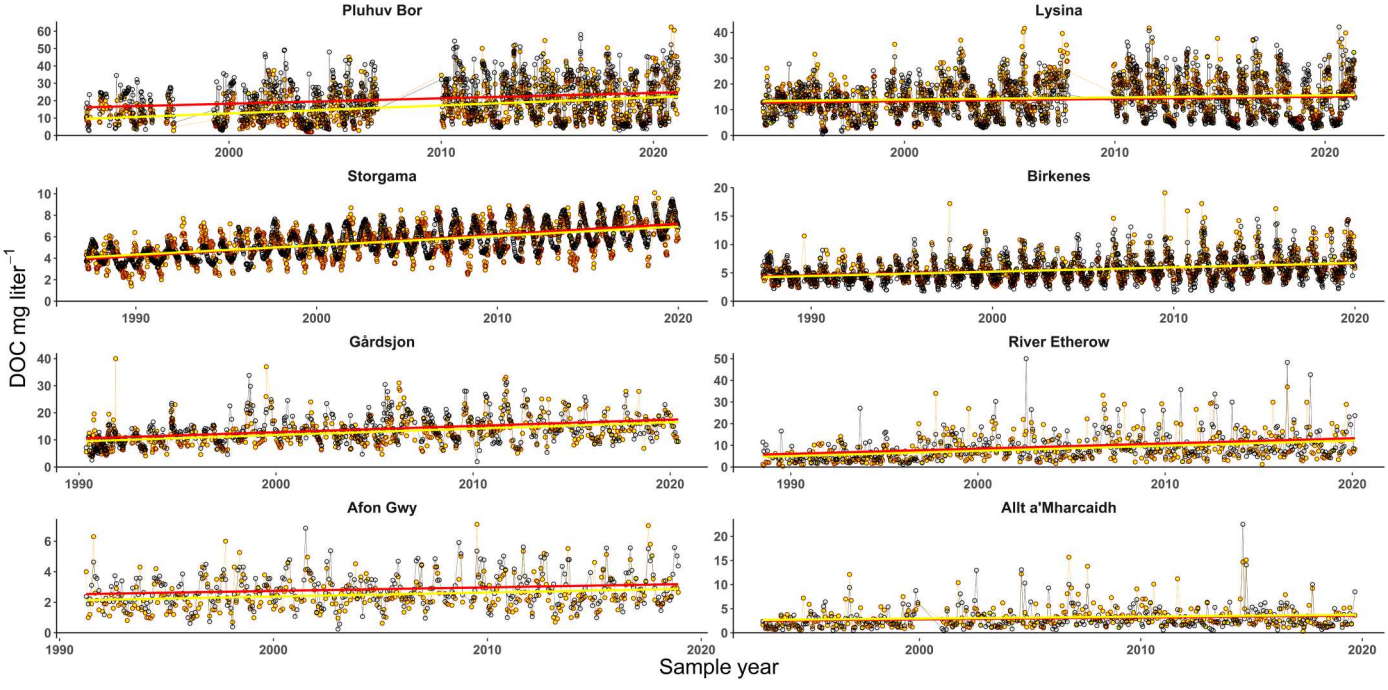

Fig. 1. Comparison of measured (yellow) and modeled (black) DOC concentration time series in a range of long-term European headwater monitoring sites. Straight lines represent linear trends in measured (yellow) and modeled (red) DOC.

Downloaded from https://www.science.org at University College London on January 23, 2023

Table 1. Key catchment characteristics and DOC simulation parameters. Window durations provide the number of days up to and including the day of collection of each DOC record over which the respective variables were averaged (or, in the case of precipitation EC, volume-weighted). Q_{10} values represent the proportional response in DOC relative to a 10°C rise in local air temperature [determined as the exponent of the temperature coefficient (α) × 10]. β_A and β_B represent nonlinear discharge effect parameters. The "discharge units and transformation" column provides the units of the original daily discharge measurements, and any multiplication factor or log transformation applied before modeling (see Materials and Methods). NA, not applicable.

Site	Catchment area (km^2)	Runoff (m)	Catchment % peat + peaty gley cover	DOC median (mg/liter)	Precipitation EC window (days)	Air temperature window (days)	Q_{10}	Discharge units and transformation	β_A	β_B	Model R^2
Storgama	0.60	0.95	0	5.5	160	60	1.25	NA	NA	NA	0.48
Gårdsjon	0.04	0.52	8	11.6	169	18	1.57	ln(liter $s^{-1} \times 10^3$)	4.10	0.92	0.46
Birkenes	0.40	1.10	2	4.9	139	11	1.52	ln(liter $s^{-1} \times 10^3$)	0.80	0.50	0.67
Afon Gwy	2.10	2.14	40	2.3	110	9	1.82	ln(m^3 $s^{-1} \times 10^3$)	4.65	1.08	0.50
Allt a'Mharcaidh	9.98	0.77	54	2.5	600	23	2.69	m^3 s^{-1}	4.40	0.85	0.47
River Etherow	13.0	1.09	90	6.8	270	16	2.23	m^3 s^{-1}	1.60	0.83	0.31
Pluhuv Bor	0.22	0.23	2	14.4	250	60	1.35	Liter s^{-1}	0.16	0.64	0.78
Lysina	0.27	0.43	6	14.0	410	74	1.28	Liter s^{-1}	0.78	0.50	0.81

effects of temperature and discharge, but Fig. 3 (D to F) shows EC to be the only variable undergoing sufficient monotonic change at any site to account for the long-term changes observed in DOC. The figure also contrasts the relative between-site consistency of the precipitation EC and temperature effects with the more variable hydrological effect, emphasizing the importance of site-specific influences of soil structure and distribution in influencing DOC flow routing and retention.

Implications for future DOC change

The inverse logarithmic relationship described by the Debye-Hückel equation, and at the center of our model, is very important with respect to recent and future DOC behavior. Under clean air policies across the European region and parts of North America, deposition of anthropogenic sulfur has fallen to levels not experienced since the early phases of the industrial revolution. Given the previously acknowledged links between acid deposition and DOC concentration, it might be assumed that DOC trends would mirror the recent flattening of the sulfur deposition trend, but increases in DOC continue to be reported (*6*), and it has been proposed that a more gradual reduction in the release of legacy pollutants from catchment soils, including anthropogenic sulfur, observed in some long-term hydrochemical records might account for the current apparent discrepancy (*33*).

It is possible that legacy effects could account for some of the variance in DOC not captured by our models, but the overall quality of the fits and their ability to account for the long-term DOC trend suggest that contemporary deposition remains the overriding factor, with soil OM solubility becoming increasingly responsive to unit reductions in the IS of precipitation as the latter fall toward background (i.e., preindustrial) levels. The concentration of DOC should, therefore, continue to rise for as long as ion deposition continues to fall, regardless how slowly, at least until pollutant deposition rates have fully stabilized (e.g., note the recent uptick in modeled change in DOC in response to changing precipitation EC in Fig. 3D).

The rising rate of change in the solubility of OM with decreasing IS, as described by the equation, may partly account for why relationships between DOC and sulfate and chloride concentration trends in spatial correlative studies of acid-sensitive waters have been found to be more acute in waters with low base cation concentrations (*4*, *6*) because such sites are likely to be more prevalent in regions receiving more dilute rainfall. However, it is also likely that the IS of water leaching soil organic layers with a naturally higher base cation content will be slightly less responsive to fluctuations in precipitation EC than the soils of most catchments included in this study, and this could lead to an overestimation of the effect of changing deposition IS on DOC concentrations in these cases. In formerly atmospherically contaminated coastal areas, including much of the western United Kingdom and southern and western Scandinavia, sea salt deposition is increasingly dominating the IS of precipitation as pollutant deposition declines (*44*). The relationship would suggest that the solubility of OM reaching upland drinking water supplies in these regions is becoming more sensitive to oscillations in soil water IS driven by fluctuations in storminess that govern sea salt inputs (*43*, *45*).

The influence of hydrology on DOC has long been recognized, and a component of recent DOC concentration trends has been attributed to increases in summer precipitation in parts of northern

Downloaded from https://www.science.org at University College London on January 23, 2023

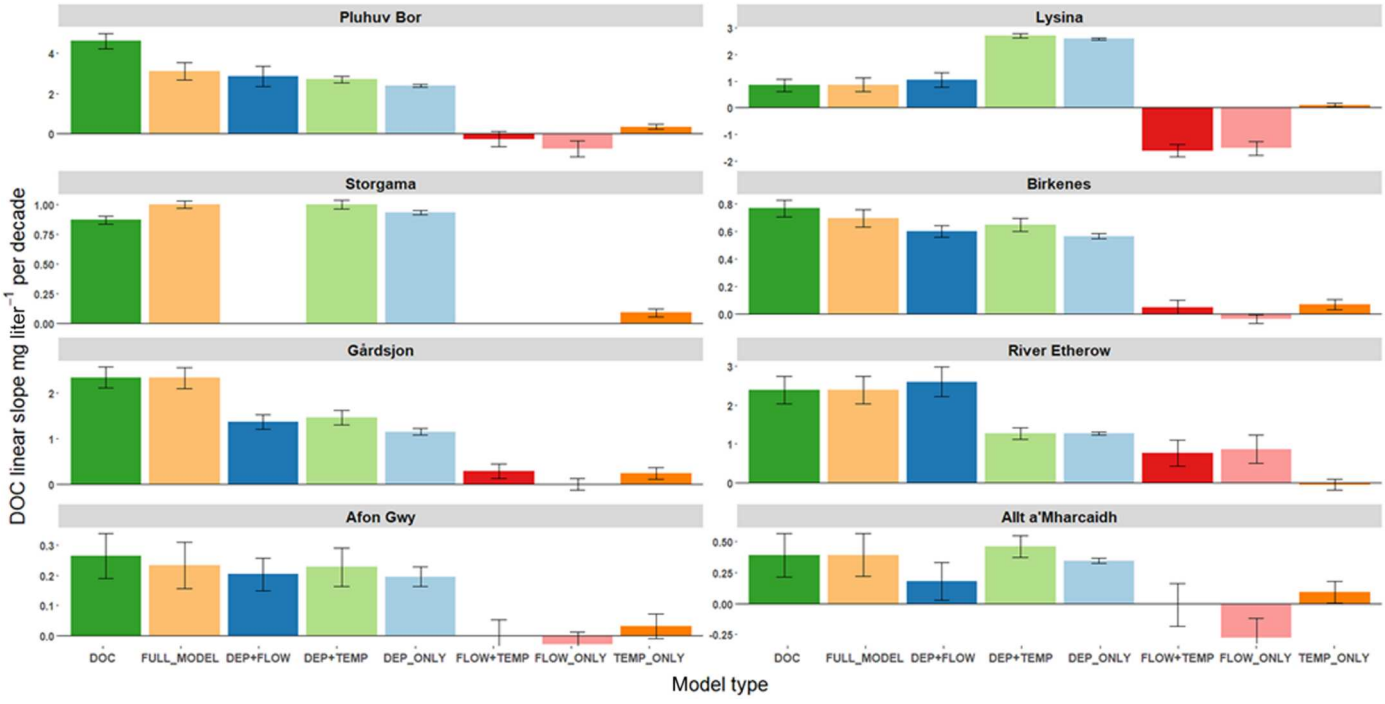

Fig. 2. Long-term linear rates of change in DOC concentration (dark green bars), compared with rates of change in modeled DOC (light orange bars), and counterfactual alternatives (other colored bars) where the effect of one or two variables in the model has been held constant. DOC, measured DOC; FULL_MODEL, DOC modeled using all parameters; DEP, FLOW, and TEMP refer to the inclusion of deposition, discharge, and temperature as dynamic variables in the counterfactual models. Error bars represent the SE of the linear trend. Discharge is not a significant predictor of DOC in Storgama, and its effects are therefore ignored.

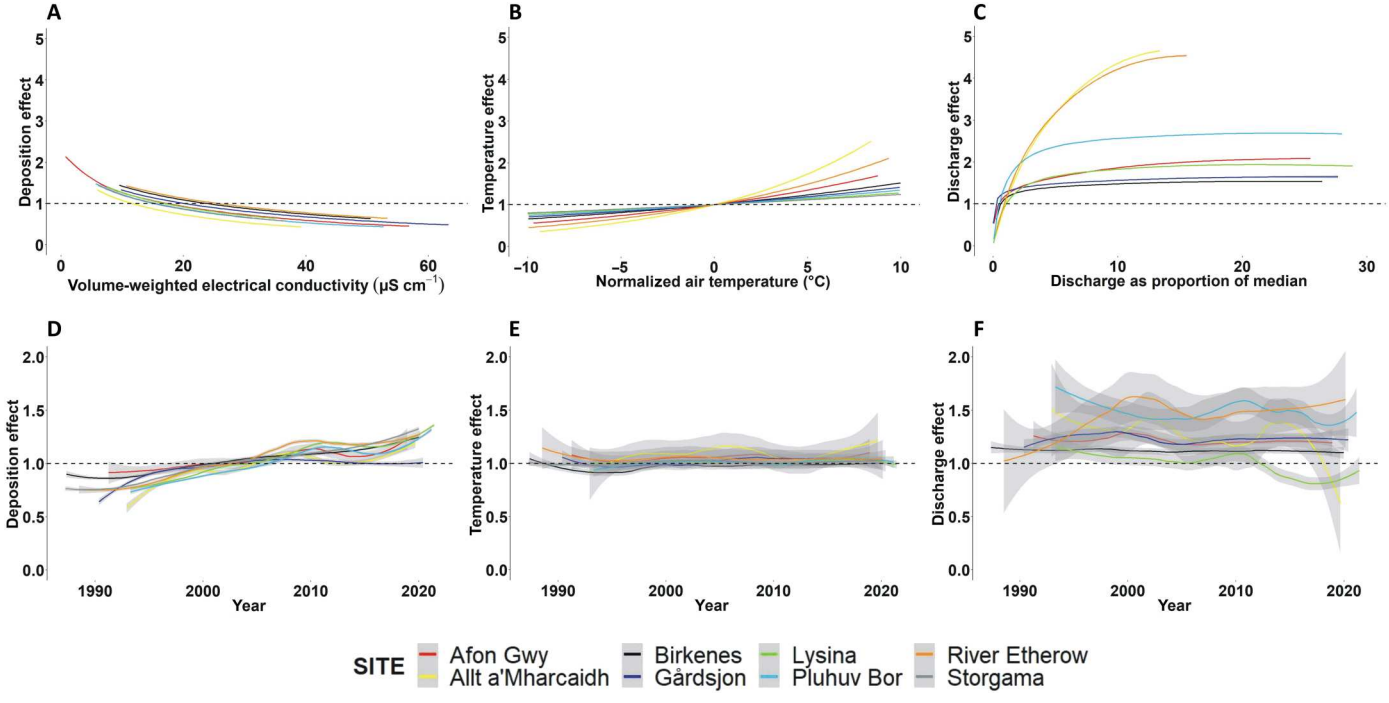

Fig. 3. Comparison of effect sizes of the three explanatory variables. Panels represent proportional change in DOC concentration (relative to site medians), with respect to the overall range of the variables (**A** to **C**) and changes over time (**D** to **F**). Trends in temporal change are represented by loess smoothers (span = 0.33).

Downloaded from https://www.science.org at University College London on January 23, 2023

Europe (*6*, *16*). Hydrology is considered to influence DOC concentrations primarily by altering flow paths, with transport of organic compounds to waters rising as runoff is increasingly routed through the most organically rich surficial horizons. The relationships between discharge and DOC represented in our simulations provide a slightly different perspective on the role of hydrology. Model fits indicate that the DOC response to increasing runoff is most acute at low discharges and that, for most sites in our study, the effect rapidly subsides as flows increase further (Fig. 3). This is perhaps more consistent, therefore, with the effect of a reduction in the proportion of dissolved OM sequestered by mineral adsorption (*24*, *25*) as the rate of drainage increases. Consequently, the widely observed tendency for DOC to rise rapidly in the early phase of storms, a feature normally attributed to the accompanying shift in flow paths, may be partly a function of the accompanying dilution of soil water IS driving an increase in OM solubility. The resulting dilution of soil water may also help explain why DOC is sometimes reported to remain high for a period after discharge has subsided to generate an apparent hysteretic effect (*46*).

The evidence for a positive thermal effect on DOC concentration is expected, given its widely reported seasonality (*47*, *48*) and observations of slight lags with air and soil temperature (*42*). However, interannual variation in air temperatures and even long-term increases projected under climate change simulations are small relative to the amplitude of the seasonal temperature cycle, and it can be difficult to detect thermal effects on DOC beyond those that can be represented by a regular annual oscillation. Despite this, we found that when the smoothed measured air temperature in the models was replaced by a sinusoidal cycle (modeled on the same temperature data), the variance explained fell by between 1 to 2%. The size of the temperature coefficients in our models implies Q_{10} temperature quotients (i.e., proportional change in DOC concentration per 10°C change in smoothed air temperature) of between 1.3 and 2.7. On the assumption that soil properties, including moisture content, remain largely unchanged, we applied the relationship between temperature constants and peat and peaty gley soil cover referred to earlier to predict the impact of future regional warming on DOC concentrations in the absence of further change in other drivers. Projected increases in European air temperatures of between 2.5° and 4.0°C by the end of the current century would be expected to drive DOC increases of between 6 to 11% for an organomineral soil-dominated catchment with a Q_{10} of 1.3, to 28 to 49% for a peat-dominated catchment with a Q_{10} of 2.7.

Implications for the spatial distribution of recent DOC change

On the basis of the support that our simulations provide for the importance of a deposition-dependent solubility control, we went on to model European-scale spatial variability in rates of change in soil OM solubility over the recent decades of clean air implementation using precipitation chemistry data drawn from the European Critical Loads dataset (*49*). The dataset provides estimates of change in deposition chemistry across a 0.50° × 0.25° grid. Computations of change in deposition EC and the inferred proportional change in DOC concentration ($[DOC]_{prop}$) for the period 1980 to 2015 were made for about 3 million sites, west of 32°E, for forest and seminatural vegetation covering about 2.3 million km^2 (Fig. 4; see the Supplementary Materials).

Despite the simplicity of the approach, the magnitude of modeled changes and their geographical distribution is highly consistent with observed rates of change in DOC concentration in European headwaters over similar time frames (*4*, *6*, *50*, *51*). Currently, the effects of hydrological and thermal change on spatial variation in DOC trends variations are not incorporated, resulting, for example, in a potential overestimation of DOC increases in the region of the Czech study sites, where a reduction in discharge has partially counteracted the effect of the precipitation IS decline. Nevertheless, our findings provide the foundation for the development of spatial predictions both past and future, integrating the effects of all three drivers, given the availability of the necessary explanatory data.

The map indicates that, between 1990 and 2015, the impacts of declining ion deposition on soil OM solubility will have been greatest in parts of central Europe and the eastern United Kingdom, where reductions in the concentration of sulfate and chloride in deposition have been particularly pronounced. The map also points to marked increases in soil OM solubility across wider areas of northern Europe, but impacts on surface waters will have been most obvious where organic soils are hydrologically connected to stream networks and where this source dominates stream DOC. Effects of deposition declines will have been least detectable where DOC is most strongly retained in mineral soils (*50*), where flow occurs largely over the soil surface (e.g., mire systems), and where urban and agricultural inputs of OM, or autochthonous DOC sources, dominate.

The modeling presented in this study therefore supports a holistic view of a set of interacting drivers, in which a thermally controlled pool of soluble OM is mobilized at a rate dependent on the IS of soil water, with the amount eventually exported to surface water dependent on flow routing and the rate of retention by any underlying mineral soil. The size of the soil organic pools may vary not only seasonally but also as a consequence of longer-term changes in soil management. For example, measures that change rates of OM delivery to the soil, e.g., by converting land from grassland to forestry (*52*) or changing the depth of soil aeration through drainage (*53*), might also be expected to influence DOC concentrations over time. Further insights may now also be gleaned into mineralization and sequestration of DOC within lakes and reservoirs, effects of various land management practices such as drainage, prescribed burning and grazing, and extreme events that are increasing in frequency and severity such as drought and wildfire.

With the significance of DOC fluxes and regional DOC increases in relation to the global carbon cycle now firmly recognized (*1*), there is an ongoing need for simple, generalizable models that can predict the response of these fluxes to global environmental change. Our study provides a basis to model the interacting influence of terrestrial OM decomposition, solubility, and transport of DOC export to the aquatic continuum and should enable improved prediction of the future response of this important carbon flux to changes in climate, land use, and the wider global carbon cycle.

MATERIALS AND METHODS

Modeling rationale

We set out to develop the most parsimonious mathematical model capable of capturing the main modes of variation in DOC

Downloaded from https://www.science.org at University College London on January 23, 2023

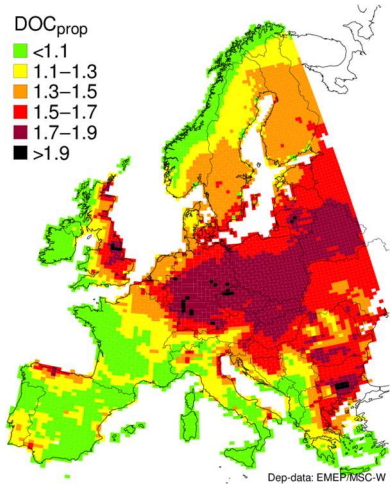

Fig. 4. Map of the estimated effect of change in the EC of precipitation (modeled using the European Critical Loads database) on proportional change in soil water DOC concentration (DOC_{prop}) between 1990 and 2015, according to the relationship between EC and DOC applied in the site-specific DOC simulations. Hydrological and temperature effects are not included.

concentrations in upland headwaters, from episodic to seasonal and multidecadal time scales. In particular, we were interested in testing the theory that DOC concentrations have been rising in many regions as a direct consequence of reductions in soil water IS (*32*, *33*), in turn driven by reductions in air pollutant deposition. To avoid overattributing, or misattributing, effects that could be due to other environmental influences, it was also necessary to represent other recognized drivers of terrestrial OM decomposition and land-to-river transport of DOC within the holistic model structure.

We assumed that soil temperature would govern the rate of microbial decomposition of recent primary production in the upper soil layers to create soluble OM and that fluctuations in air temperature would provide a robust surrogate for soil temperature variation, particularly when averaged over multiple days. We also reasoned that the proportion of the DOC mobilized in the soil water that is ultimately transported to the surface water would be dependent on hydrological conditions at the time of sampling, which in turn could be represented by instantaneous stream discharge.

Our primary focus, however, was to test whether the Debye-Hückel limiting law (*40*) could be applied to represent the effect of fluctuations in soil water IS on soil OM solubility. Debye-Hückel theory suggests that the solubility of humic substances in soil solution should increase with any reduction in solute strength, as the diffuse double layer around organic colloids expands and the charge shielding that promotes coagulation is consequently reduced. To some extent, fluctuations in soil pH and soil water IS are intrinsically linked. For example, reductions in IS at electrolytic concentrations typical of boreal forest soils across realistic gradients of acid deposition can also raise soil pH (*54*), although modeling of responses suggests that some of the most important groups of strong organic acids remain in solution across broad pH ranges (*33*, *55*, *56*). Because of the paucity of long-term soil water chemistry records that could be linked to most of the headwater catchments of interest, we instead gathered records of precipitation chemistry measured in samples from local bulk collectors. While precipitation monitoring protocols have not always covered the full range of ions necessary to compute IS, the monitoring of the specific EC of precipitation, which correlates very tightly with IS, is routine and analytically robust and therefore provides the best opportunity for assessing evidence for a direct effect of deposition IS on DOC concentrations.

Sites

We identified eight long-term headwater stream monitoring stations drawn from national or regional monitoring programs in the Czech Republic, Norway, Sweden, and the United Kingdom, for which frequent (i.e., at least monthly) DOC measurements were available, together with local records for daily stream discharge, bulk precipitation EC (at least monthly), and either measured or modeled (i.e., 1-km resolution) daily air temperature, covering a period of at least 25 years (table S1).

Stream water and bulk precipitation chemical analysis

Streamwater samples were filtered through 0.45-μm cellulose nitrate filters and analyzed for DOC using Total Organic Carbon (TOC) analyzers by first acidifying samples to purge inorganic carbon, followed by high-temperature combustion and spectrometric analysis of the resulting CO_2. Temperature-standardized (either 20° or 25°C) EC of precipitation samples was measured at nearby precipitation chemistry monitoring stations.

Meteorological data

Daily mean air temperature records were obtained either from local meteorological stations or, in the case of the U.K. sites, using daily 1-km resolution interpolated data provided by the Climate Hydrology and Ecology research Support System (CHESS) meteorology dataset for Great Britain (*57*). The amount of precipitation collected for each precipitation chemistry sample was used to determine precipitation-weighted EC estimates.

Model development

DOC concentrations were modeled on a site-specific basis using a common iterative fitting approach according to the following steps.

Step 1

DOC concentrations were converted to proportions of site median concentrations ($[DOC]_{prop}$) and then natural log-transformed ($ln[DOC]_{prop}$) to achieve approximately normal distributions. Debye-Hückel theory implies that the natural logarithm of ion activity in dilute solutions is inversely proportional to the square root of IS. We assumed as our starting point, therefore, that providing the average charge density of the organic compounds had not changed significantly over time; change in $ln[DOC]_{prop}$ would be related to change in precipitation EC when also expressed in proportional terms (i.e., EC_{prop}) as follows

$$ln[DOC]_{prop} = 1 - \sqrt{EC_{prop}} \quad (1)$$

where EC_{prop} represents precipitation EC volume-weighted over a site-specific antecedent period.

For each site, we initially determined mean precipitation EC, weighted by precipitation amount, for 365 days antecedent to the collection of each DOC measurement and divided this by the median of all annual precipitation-weighted precipitation values to provide EC_{prop}. We then applied Eq. 1 and varied the antecedent

Downloaded from https://www.science.org at University College London on January 23, 2023

smoothing period in 10-day increments until we maximized the variance in $ln[DOC]_{prop}$ explained.

Step 2

Daily mean air temperatures for each site were normalized by subtracting the long-term mean. The seasonal pattern in the $ln[DOC]_{prop}$ residuals from Eq. 1, assuming this to represent the effect of temperature-dependent decomposition on soluble OM production, was modeled using sine and cosine functions applied to the day of the year. We then determined the number of days (before the day of each DOC sample) that daily mean air temperature values would need to be averaged over for the annual peaks in the smoothed air temperature records and the modeled seasonal cycle of Eq. 1 residuals to align. Regression of the $ln[DOC]_{prop}$ residuals against the smoothed normalized air temperature data provided an initial temperature coefficient.

Step 3

Exploratory data analysis had shown that while DOC appeared to vary logarithmically with both precipitation EC and temperature, relationships with discharge were either relatively linear, or DOC varied with the logarithm of discharge. We therefore next determined the exponents of the residuals from the step 2 model (i.e., EC + temperature) before plotting them against instantaneous discharge or the logarithm of discharge. In the case of the Storgama site, we observed no obvious relationship between the step 2 model residuals and discharge and therefore did not include a discharge variable in the final Storgama DOC model.

For the remaining seven sites, we observed asymptotic relationships, with the step 2 model residuals not only increasing but also leveling off at moderate to high discharges. These relationships were most effectively described by the following function

$$\text{Discharge effect } (\beta) = \frac{1}{\frac{\beta_A}{Q} - \beta_B + 1} \quad (2)$$

where β_A and β_B are constants and Q is either the instantaneous discharge or the natural logarithm of instantaneous discharge, depending on the site. While not necessary for the datasets used in our study, it would be necessary to add a small constant to Q before log transformation should the Q range include values of 1 or less (regardless of units) to ensure that all transformed values are positive. Initial values for β_A and β_B were established using the Microsoft Excel "Solver" application to explain the step 2 model residuals.

Step 4

Because the modeled IS and thermal effects were logarithmic, the full simulation model took the following form

$$[DOC]_t = [DOC]_{\text{median}} \cdot \exp\left(1 - \sqrt{\frac{EC_t}{EC_{\text{median}}}} + \alpha T_t\right) \cdot \frac{1}{\frac{\beta_A}{Q_t} - \beta_B + 1} \quad (3)$$

where $[DOC]_t$ is the DOC concentration of runoff of a site at time t and $[DOC]_{\text{median}}$ is the long-term site median DOC concentration. Likewise, EC_t represents the EC of bulk precipitation, precipitation-weighted over a site-specific period antecedent to time t, while EC_{median} represents the median of the daily computed precipitation-weighted EC_t values. The term T_t represents the normalized daily mean air temperature averaged over a site-specific number of days antecedent to time t, and the coefficient α represents the effect of the smoothed temperature variable. Last, Q_t represents discharge, or the natural logarithm of discharge, depending on the site, on the day of water sampling, with the β coefficients determined according to Eq. 2.

Step 5

The final site-specific model calibration involved the iterative adjustment of smoothing windows for air temperature and precipitation EC, the air temperature (α), and the discharge coefficients (β_A and β_B) to maximize the final variance in measured [*DOC*] explained while also ensuring that the linear slopes of the modeled and observed DOC trends were in approximate agreement. The final site-specific model smoothing windows and variable coefficients for each site are indicated in Table 1 (coefficient α = the natural logarithm of the temperature quotient $Q_{10}/10$).

Model structure exploration

To consider the relative contributions of the three explanatory variables to the observed long-term DOC trends at the study sites (as presented in Figs. 2 and 3), we simply nullified the influence of one or two of the variables within Eq. 3, such that the term $\sqrt{\frac{EC_t}{EC_{\text{median}}}}$ was replaced with 1, while the discharge and temperature terms were removed, as appropriate. Rates of change (with time) in observed DOC, modeled DOC according to Eq.3, and modeled DOC with one or two variables omitted, were determined by linear regression.

Spatial modeling of the effect of the changing EC of precipitation

To consider the implications of our field observations for change in soil OM solubility at a continental scale, we applied the European Background Database (EU-DB) (*49*) to determine regional-scale change in bulk precipitation EC over the period for which data were available (i.e., 1990–2015). Computations of precipitation EC and the inferred proportional change in DOC (DOC_{prop}) in runoff were made for about 3 million sites in Europe, west of 32°E, for forest and seminatural vegetation (EUNIS classes D through G), covering about 2.3 million km^2.

Bulk precipitation EC (in μS/cm) was computed from the concentrations of the ions present as

$$EC = \sum_{i=1}^{n} \Lambda_i^0 [X_i] \quad (4)$$

where $[X_i]$ is the concentration of ion i (in eq/m^3), $\Lambda^0{}_i$ is the (limiting) equivalent conductivity of ion i (in Scm^2/eq), and n the number of ions.

We considered the following ions (charges suppressed): base cations, i.e.,

$$[BC] = [Ca] + [Mg] + [K] + [Na] \quad (5)$$

Note that gradual long-term reductions in base cation deposition are known to have occurred, but neither long-term records nor modeled estimates of change were available for the European region. Consequently, base cation deposition for the year 2000 was derived from modeling conducted by van Loon *et al.* (*58*) and held constant for the full time series and the "pollutants" sulfate, [SO_4], nitrate [NO_3] and ammonium [NH_4], and chloride [Cl].

Downloaded from https://www.science.org at University College London on January 23, 2023

The bicarbonate concentration [HCO_3] was computed from the proton concentration, [H], as

$$[HCO_3] = K_{HCO_3}/[H] \quad (6)$$

where K_{HCO3} is the equilibrium constant. [H] itself was then computed from the charge balance

$$[H] - [HCO_3] + [ANC] = 0 \quad (7)$$

with the ANC (acid-neutralizing capacity) defined as

$$[ANC] = [BC] - [Cl] - [SO_4] - [NO_3] + [NH_4] \quad (8)$$

Equation 7 becomes a quadratic equation in [H] after inserting Eq. 6, and the (only positive) solution is

$$[H] = \frac{1}{2}\left(\sqrt{[ANC]^2 + 4K_{HCO_3}} - [ANC]\right) \quad (9)$$

We define the following property, DOC_{prop}, as

$$DOC_{prop} = \exp\left(1 - \sqrt{EC_{2015}/EC_{1990}}\right) \quad (10)$$

where EC_{1990} and EC_{2015} are the conductivities computed with N- and S-depositions from the years 1990 and 2015, respectively.

Using data from the European Background Database, the concentrations of ion X were computed from its wet deposition flux, X_{wet}, as follows

$$[X] = X_{wet}/P \quad (11)$$

where P is the annual precipitation.

Figure S1 presents the grid average wet deposition ratio used in the calculations. Figure S2 shows the cumulative distribution functions (cdfs) of EC (see Eq. 4) for two deposition years (1990 and 2015) for all sites west of 32°E (about 3 million sites). It also shows that, for example, the 90th percentile in 2015 is around 20 μS cm^{-1} in 2015 and above 80 μS cm^{-1} in 1990. Median EC values are mapped in fig. S3. Figure S4 provides the cdfs of DOC_{prop} for all sites, while the spatial distribution of the DOC_{prop} values (see Eq. 10) of all sites can be seen in the maps in fig. S5.

Supplementary Materials

This PDF file includes:

Figs. S1 to S6
Table S1

REFERENCES AND NOTES

1. T. J. Battin, S. Luyssaert, L. A. Kaplan, A. K. Aufdenkampe, A. Richter, L. J. Tranvik, The boundless carbon cycle. *Nat. Geosci.* **2**, 598–600 (2009).
2. J. Settele, R. Scholes, R. Betts, S. E. Bunn, P. Leadley, D. Nepstad, J. T. Overpeck, M. A. Taboada, "Terrestrial and inland water systems" in *Climate Change 2014: Impacts, Adaptation, and Vulnerability. Part A: Global and Sectoral Aspects. Contribution of Working Group II to the Fifth Assessment Report of the Intergovernmental Panel of Climate Change*, C. B. Field, V. R. Barros, D. J. Dokken, K. J. Mach, M. D. Mastrandrea, T. E. Bilir, M. Chatterjee, K. L. Ebi, Y. O. Estrada, R. C. Genova, B. Girma, E. S. Kissel, A. N. Levy, S. MacCracken, P. R. Mastrandrea, L. L. White, Eds. (Cambridge University Press, 2014), pp. 271–359.
3. P. Ciais, A. V. Borges, G. Abril, M. Meybeck, G. Folberth, D. Hauglustaine, I. A. Janssens, The impact of lateral carbon fluxes on the European carbon balance. *Biogeosciences* **5**, 1259–1271 (2008).
4. D. T. Monteith, J. L. Stoddard, C. D. Evans, H. A. de Wit, M. Forsius, T. Høgåsen, A. Wilander, B. L. Skjelkvåle, D. S. Jeffries, J. Vuorenmaa, B. Keller, J. Kopácek, J. Vesely, Dissolved organic carbon trends resulting from changes in atmospheric deposition chemistry. *Nature* **450**, 537–540 (2007).
5. Ø. A. Garmo, B. L. Skjelkvåle, H. A. de Wit, L. Colombo, C. Curtis, J. Fölster, A. Hoffmann, J. Hruška, T. Høgåsen, D. S. Jeffries, W. B. Keller, P. Krám, V. Majer, D. T. Monteith, A. M. Paterson, M. Rogora, D. Rzychon, S. Steingruber, J. L. Stoddard, J. Vuorenmaa, A. Worsztynowicz, Trends in surface water chemistry in acidified areas in Europe and North America from 1990 to 2008. *Water, Air, Soil Pollut.* **225**, 1880 (2014).
6. H. A. de Wit, J. L. Stoddard, D. T. Monteith, J. E. Sample, K. Austnes, S. Couture, J. Fölster, S. N. Higgins, D. Houle, J. Hruška, P. Krám, J. Kopáček, A. M. Paterson, S. Valinia, H. V. Dam, J. Vuorenmaa, C. D. Evans, Cleaner air reveals growing influence of climate on dissolved organic carbon trends in northern headwaters. *Environ. Res. Lett.* **16**, 104009 (2021).
7. F. Guillemette, S. L. McCallister, P. A. del Giorgio, Differentiating the degradation dynamics of algal and terrestrial carbon within complex natural dissolved organic carbon in temperate lakes. *J. Geophys. Res. Biogeo.* **118**, 963–973 (2013).
8. J.-E. Thrane, D. O. Hessen, T. Andersen, The absorption of light in lakes: Negative impact of dissolved organic carbon on primary productivity. *Ecosystems* **17**, 1040–1052 (2014).
9. J. P. Ritson, N. J. D. Graham, M. R. Templeton, J. M. Clark, R. Gough, C. Freeman, The impact of climate change on the treatability of dissolved organic matter (DOM) in upland water supplies: A UK perspective. *Sci. Total Environ.* **473-474**, 714–730 (2014).
10. M. Camino-Serrano, B. Guenet, S. Luyssaert, P. Ciais, V. Bastrikov, B. De Vos, B. Gielen, G. Gleixner, A. Jornet-Puig, K. Kaiser, D. Kothawala, R. Lauerwald, J. Peñuelas, M. Schrumpf, S. Vicca, N. Vuichard, D. Walmsley, I. A. Janssens, ORCHIDEE-SOM: Modeling soil organic carbon (SOC) and dissolved organic carbon (DOC) dynamics along vertical soil profiles in Europe. *Geosci. Model Dev.* **11**, 937–957 (2018).
11. M. N. Futter, D. Butterfield, B. J. Cosby, P. J. Dillon, A. J. Wade, P. G. Whitehead, Modeling the mechanisms that control in-stream dissolved organic carbon dynamics in upland and forested catchments. *Water Resour. Res.* **43**, (2007).
12. C. Liao, Q. Zhuang, L. R. Leung, L. Guo, Quantifying dissolved organic carbon dynamics using a three-dimensional terrestrial ecosystem model at high spatial-temporal resolutions. *J. Adv. Model. Earth Syst.* **11**, 4489–4512 (2019).
13. M. N. Futter, S. Löfgren, S. J. Köhler, L. Lundin, F. Moldan, L. Bringmark, Simulating dissolved organic carbon dynamics at the Swedish Integrated Monitoring Sites with the Integrated Catchments Model for Carbon, INCA-C. *Ambio.* **40**, 906–919 (2011).
14. E. C. Rowe, E. Tipping, M. Posch, F. Oulehle, D. M. Cooper, T. G. Jones, A. Burden, J. Hall, C. D. Evans, Predicting nitrogen and acidity effects on long-term dynamics of dissolved organic matter. *Environ. Pollut.* **184**, 271–282 (2014).
15. H. A. De Wit, J. Mulder, A. Hindar, L. Hole, Long-term increase in dissolved organic carbon in streamwaters in Norway is response to reduced acid deposition. *Environ. Sci. Technol.* **41**, 7706–7713 (2007).
16. M. Erlandsson, I. Buffam, J. Fölster, H. Laudon, J. Temnerud, G. A. Weyhenmeyer, K. Bishop, Thirty-five years of synchrony in the organic matter concentrations of Swedish rivers explained by variation in flow and sulphate. *Glob. Change Biol.* **14**, 1191–1198 (2008).
17. E. M. Thurman, *Organic Geochemistry of Natural Waters* (Martinus Nijhoff/Dr W. Junk Publishers, 1985).
18. E. Tipping, M. F. Billett, C. L. Bryant, S. Buckingham, S. A. Thacker, Sources and ages of dissolved organic matter in peatland streams: Evidence from chemistry mixture modelling and radiocarbon data. *Biogeochemistry* **100**, 121–137 (2010).
19. C. D. Evans, C. Freeman, L. G. Cork, D. N. Thomas, B. Reynolds, M. F. Billett, M. H. Garnett, D. Norris, Evidence against recent climate-induced destabilisation of soil carbon from ^{14}C analysis of riverine dissolved organic matter. *Geophys. Res. Lett.* **34**, L07407 (2007).
20. M. U. F. Kirschbaum, The temperature dependence of soil organic matter decomposition, and the effect of global warming on soil organic C storage. *Soil Biol. Biochem.* **27**, 753–760 (1995).
21. E. A. Davidson, I. A. Janssens, Temperature sensitivity of soil carbon decomposition and feedbacks to climate change. *Nature* **440**, 165–173 (2006).
22. G. M. Hornberger, K. E. Bencala, D. M. McKnight, Hydrological controls on dissolved organic carbon during snowmelt in the snake river near Montezuma, Colorado. *Biogeochemistry* **25**, 147–165 (1994).
23. H. Wen, J. Perdrial, B. W. Abbott, S. Bernal, R. Dupas, S. E. Godsey, A. Harpold, D. Rizzo, K. Underwood, T. Adler, G. Sterle, L. Li, Temperature controls production but hydrology regulates export of dissolved organic carbon at the catchment scale. *Hydrol. Earth Syst. Sci.* **24**, 945–966 (2020).
24. K. Kaiser, K. Kalbitz, Cycling downwards - dissolved organic matter in soils. *Soil Biol. Biochem.* **52**, 29–32 (2012).
25. K. Kaiser, G. Guggenberger, W. Zech, Sorption of DOM and DOM fractions to forest soils. *Geoderma* **74**, 281–303 (1996).
26. E. Tipping, M. A. Hurley, A model of solid-solution interactions in acid organic soils, based on the complexation properties of humic substances. *J. Soil Sci.* **39**, 505–519 (1988).

Downloaded from https://www.science.org at University College London on January 23, 2023

27. M. H. B. Hayes, R. S. Swift, "The chemistry of soil organic colloids" in *The Chemistry of Organic Constituents* (John Wiley & Sons, 1978), pp. 179–320.
28. C. D. Evans, T. G. Jones, A. Burden, N. Ostle, P. Zieliński, M. D. A. Cooper, M. Peacock, J. M. Clark, F. Oulehle, D. Cooper, C. Freeman, Acidity controls on dissolved organic carbon mobility in organic soils. *Glob. Change Biol.* **18**, 3317–3331 (2012).
29. S. M. Ekström, E. S. Kritzberg, D. B. Kleja, N. Larsson, P. A. Nilsson, W. Graneli, B. Bergkvist, Effect of acid deposition on quantity and quality of dissolved organic matter in soil-water. *Environ. Sci. Technol.* **45**, 4733–4739 (2011).
30. J. Kennedy, M. F. Billett, D. Duthie, A. R. Fraser, A. F. Harrison, Organic matter retention in an upland humic podzol; The effects of pH and solute type. *Eur. J. Soil Sci.* **47**, 615–625 (1996).
31. G. F. Vance, M. B. David, Effect of acid treatment on dissolved organic carbon retention by a spodic horizon. *Soil Sci. Soc. Am. J.* **53**, 1242–1247 (1989).
32. J. Hruska, P. Kram, W. H. McDowell, F. Oulehle, Increased dissolved organic carbon (DOC) in Central European streams is driven by reductions in ionic strength rather than climate change or decreasing acidity. *Environ. Sci. Technol.* **43**, 4320–4326 (2009).
33. G. B. Lawrence, K. M. Roy, Ongoing increases in dissolved organic carbon are sustained by decreases in ionic strength rather than decreased acidity in waters recovering from acidic deposition. *Sci. Total Environ.* **766**, 142529 (2021).
34. R. L. Hale, S. E. Godsey, Dynamic stream network intermittence explains emergent dissolved organic carbon chemostasis in headwaters. *Hydrol. Process.* **33**, 1926–1936 (2019).
35. J. Lee, P. G. Whitehead, M. N. Futter, J. W. Hall, Impacts of droughts and acidic deposition on long-term surface water dissolved organic carbon concentrations in upland Catchments in Wales. *Front. Environ. Sci.* **8**, 10.3389/fenvs.2020.578611, (2020).
36. X. Wei, D. J. Hayes, I. Fernandez, S. Fraver, J. Zhao, A. Weiskittel, Climate and atmospheric deposition drive the inter-annual variability and long-term trend of dissolved organic carbon flux in the conterminous United States. *Sci. Total Environ.* **771**, 145448 (2021).
37. A. Lepistö, M. N. Futter, P. Kortelainen, Almost 50 years of monitoring shows that climate, not forestry, controls long-term organic carbon fluxes in a large boreal watershed. *Glob. Change Biol.* **20**, 1225–1237 (2014).
38. L. J. Hall, E. J. S. Emilson, B. Edwards, S. A. Watmough, Patterns and trends in lake concentrations of dissolved organic carbon in a landscape recovering from environmental degradation and widespread acidification. *Sci. Total Environ.* **765**, 142679 (2021).
39. T. Rosset, S. Binet, F. Rigal, L. Gandois, Peatland dissolved organic carbon export to surface waters: Global significance and effects of anthropogenic disturbance. *Geophys. Res. Lett.* **49**, e2021GL096616 (2022).
40. P. . Debye, E. . Hückel, The theory of electrolytes. I. Freezing point depression and related phenomena. *Physikalische Zeitschrift.* **24**, 185–206 (1923).
41. R. Bracho, S. Natali, E. Pegoraro, K. G. Crummer, C. Schädel, G. Celis, L. Hale, L. Wu, H. Yin, J. M. Tiedje, K. T. Konstantinidis, Y. Luo, J. Zhou, E. A. G. Schuur, Temperature sensitivity of organic matter decomposition of permafrost-region soils during laboratory incubations. *Soil Biol. Biochem.* **97**, 1–14 (2016).
42. J. M. Clark, D. Ashley, M. Wagner, P. J. Chapman, S. N. Lane, C. D. Evans, A. L. Heathwaite, Increased temperature sensitivity of net DOC production from ombrotrophic peat due to water table draw-down. *Glob. Change Biol.* **15**, 794–807 (2009).
43. H. A. de Wit, R. F. Wright, Projected stream water fluxes of NO_3 and total organic carbon from the Storgama headwater catchment, Norway, under climate change and reduced acid deposition. *Ambio* **37**, 56–63 (2008).
44. C.-H. M. Tso, D. Monteith, T. Scott, H. Watson, B. Dodd, M. G. Pereira, P. Henrys, M. Hollaway, S. Rennie, A. Lowther, J. Watkins, R. Killick, G. Blair, The evolving role of weather types on rainfall chemistry under large reductions in pollutant emissions. *Environ. Pollut.* **299**, 118905 (2022).
45. C. D. Evans, D. T. Monteith, D. M. Cooper, Long-term increases in surface water dissolved organic carbon: Observations, possible causes and environmental impacts. *Environ. Pollut.* **137**, 55–71 (2005).
46. S. Wagner, J. H. Fair, S. Matt, J. D. Hosen, P. Raymond, J. Saiers, J. B. Shanley, T. Dittmar, A. Stubbins, Molecular hysteresis: Hydrologically driven changes in riverine dissolved organic matter chemistry during a storm event. *J. Geophys. Res. Biogeo.* **124**, 759–774 (2019).
47. J. J. C. Dawson, C. Soulsby, D. Tetzlaff, M. Hrachowitz, S. M. Dunn, I. A. Malcolm, Influence of hydrology and seasonality on DOC exports from three contrasting upland catchments. *Biogeochemistry* **90**, 93–113 (2008).
48. A. F. Harrison, K. Taylor, A. Scott, J. Poskitt, D. Benham, J. Grace, J. Chaplow, P. Rowland, Potential effects of climate change on DOC release from three different soil types on the Northern Pennines UK: Examination using field manipulation experiments. *Glob. Change Biol.* **14**, 687–702 (2008).
49. M. Posch, G. J. Reinds, The European Background Database of N and S critical loads, in *European Critical Loads: Database, Biodiversity and Ecosystems at Risk: CCE Final Report 2017*, Hettelingh, J.-P., Posch, M., Slootweg, J., Eds. (RIVM Report 2017-0155, Bilthoven, 2017, 2017), pp. 49–63.
50. F. Oulehle, J. Hruška, Rising trends of dissolved organic matter in drinking-water reservoirs as a result of recovery from acidification in the Ore Mts., Czech Republic. *Environ. Pollut.* **157**, 3433–3439 (2009).
51. C. Sucker, K. von Wilpert, H. Puhlmann, Acidification reversal in low mountain range streams of Germany. *Environ. Monit. Assess.* **174**, 65–89 (2011).
52. E. S. Kritzberg, Centennial-long trends of lake browning show major effect of afforestation. *Limnol. Oceanogr. Lett.* **2**, 105–112 (2017).
53. F. Worrall, A. Armstrong, J. Holden, Short-term impact of peat drain-blocking on water colour, dissolved organic carbon concentration, and water table depth. *J. Hydrol.* **337**, 315–325 (2007).
54. D. D. Richter, P. J. Comer, K. S. King, H. S. Sawin, D. S. Wright, Effects of low ionic strength solutions on pH of acid forested soils. *Soil Sci. Soc. Am. J.* **52**, 261–264 (1988).
55. H. Fakhraei, C. T. Driscoll, Proton and aluminum binding properties of organic acids in surface waters of the Northeastern U.S. *Environ. Sci. Technol.* **49**, 2939–2947 (2015).
56. J. Hruška, S. Köhler, H. Laudon, K. Bishop, Is a universal model of organic acidity possible: Comparison of the acid/base properties of dissolved organic carbon in the boreal and temperate zones. *Environ. Sci. Technol.* **37**, 1726–1730 (2003).
57. E. L.Robinson, E. Blyth, D. B.Clark, E. Comyn-Platt, J. Finch, A. C. Rudd, *Climate Hydrology and Ecology Research Support System Meteorology Dataset for Great Britain (1961–2012) [CHESS-met] v1.2* (NERC Environmental Information Data Centre, 2017); https://doi.org/10.5285/b745e7b1-626c-4ccc-ac27-56582e77b900.
58. M. van Loon, L. Tarrasón, M. Posch, *Modelling Base Cations in Europe* (Report to the Working Group on Effects MSC-W 2/2005 Technical report, Norwegian Meteorological Institute, 2005), p. 58.

Acknowledgments: We thank G. Jan Reinds from Wageningen Environmental Research (NL) for his contribution in preparing the databases used to produce Fig. 4 and the Trust Fund for the effect-oriented activities under the Convention on Long-range Transboundary Air Pollution. We also thank W. Aas, NILU, of the Norwegian Institute for Air Research (NILU) for provision of Norwegian deposition chemistry data. **Funding:** This study was supported by the Natural Environment Research Council (NERC) under the projects FREEDOM (NE/R009198/1) and FREEDOM-BCCR (NE/S016937/2) and the National Capability programs LOCATE (NEC05686) and UK-SCAPE (NE/R016429/1). Several national long-term monitoring programs, funded by regional governments, environment institutes and conservation agencies, contributed data. The UK Upland Waters Monitoring Network (UWMN) is, or has been, supported by the UK Department for Environment Food and Rural Affairs (DEFRA), the U.K. Centre for Ecology & Hydrology, the Department of the Environment (Northern Ireland), the Environment Agency (EA), the Forestry Commission (FC), Natural Resources Wales (NRW), the Scottish Environmental Protection Agency (SEPA), Nature Scot (NS), the Welsh Government, the Scottish Government through Marine Scotland Science Pitlochry, Queen Mary University of London, the Environmental Change Research Centre, University College London, and volunteer samplers. River Etherow monitoring is currently supported by Moors for the Future through funding from Yorkshire Water, United Utilities, and Severn Trent Water. Daily mean river flow data for U.K. sites were obtained from the U.K. National River Flow Archive and U.K. precipitation data from the Defra-funded Precip-Net. Contributions from the Czech Republic were made under project 21-22810J funded by Czech Science Foundation. The Norwegian Environment Agency funded the Norwegian monitoring program for surface water quality. **Author contributions:** Conceptualization: D.T.M. Methodology: D.T.M. and M.P. Writing (original draft): D.T.M., M.P., and C.D.E. Writing (review and editing): D.T.M., M.P., C.D.E., P.A.H., H.A.d.W., J.H., P.K., F.M., A.R., J.L.S., E.M.S., and M.G.P. **Competing interests:** The authors declare that they have no competing interests. **Data and materials availability:** Data used in the production of this paper are drawn from a large number of national and local sources listed in table S1. All data needed to evaluate the conclusions in the paper are present in the paper, the Supplementary Materials, or a dataset to be made available online via the Zenodo web-platform (zenodo.org; 10.5281/zenodo.7410366).

Submitted 11 August 2022
Accepted 16 December 2022
Published 18 January 2023
10.1126/sciadv.ade3491

Downloaded from https://www.science.org at University College London on January 23, 2023

ScienceAdvances

Long-term rise in riverine dissolved organic carbon concentration is predicted by electrolyte solubility theory

Donald T. Monteith, Peter A. Henrys, Jakub Hruka, Heleen A. de Wit, Pavel Krm, Filip Moldan, Maximilian Posch, Antti Rike, John L. Stoddard, Ewan M. Shilland, M. Gloria Pereira, and Chris D. Evans

Sci. Adv., **9** (3), eade3491.
DOI: 10.1126/sciadv.ade3491

View the article online
https://www.science.org/doi/10.1126/sciadv.ade3491
Permissions
https://www.science.org/help/reprints-and-permissions

Downloaded from https://www.science.org at University College London on January 23, 2023

Use of this article is subject to the Terms of service

Science Advances (ISSN) is published by the American Association for the Advancement of Science. 1200 New York Avenue NW, Washington, DC 20005. The title *Science Advances* is a registered trademark of AAAS.
Copyright © 2023 The Authors, some rights reserved; exclusive licensee American Association for the Advancement of Science. No claim to original U.S. Government Works. Distributed under a Creative Commons Attribution License 4.0 (CC BY).